Chemical Physics Letters 467 (2009) 398–401

Contents lists available at ScienceDirect

Chemical Physics Letters

journal homepage: www.elsevier.com/locate/cplett

# 'Ex situ' magnetic resonance volume imaging

Vasiliki Demas [a,b,c,*], John M. Franck [a,b], Louis S. Bouchard [d], Dimitris Sakellariou [e], Carlos A. Meriles [f], Rachel Martin [g], Pablo J. Prado [c,h], Alejandro Bussandri [h], Jeffrey A. Reimer [a,b], Alex Pines [a,b]

[a] University of California-Berkeley, Departments of Chemistry and Chemical Engineering, Berkeley, CA 94720, United States
[b] Lawrence Berkeley National Laboratory, MSD and EETD Divisions, Berkeley, CA 94720, United States
[c] T2 Biosystems, System Development, 286 Cardinal Medeiros Ave., Cambridge, MA 02141, United States
[d] University of California-Los Angeles, Department of Chemistry and Biochemistry, Los Angeles, CA 90095, United States
[e] Commissariat a l'Energie Atomique in Saclay, 91191 Gif-sur-Yvette Cedex, France
[f] City College of New York, Department of Physics, New York, NY 10031, United States
[g] University of California-Irvine, Department of Chemistry, Irvine, CA 92697, United States
[h] Quantum Magnetics (currently GE Security), 15175 Innovation Dr., San Diego, CA 92128, United States

ARTICLE INFO

*Article history:*
Received 27 June 2008
In final form 7 November 2008
Available online 27 November 2008

ABSTRACT

The portable NMR community has introduced advances that have allowed for a variety of studies. Imaging of static and moving objects has almost become standardized. The inherent static field gradients of portable systems have, however, limited such studies to imaging of slices perpendicular to the main gradient; full volume imaging in transportable, open systems has not been actively pursued. We present a true three-dimensional image of a phantom in an ex situ, electromagnet-based system. The basic concepts and designs put forth here extend in a straightforward fashion to higher fields and imaging of larger samples by ex situ methodologies.



## 1. Introduction

Ex situ (i.e. single sided, and/or portable) magnetic resonance (MR) volume imaging could potentially apply MR to several new areas; most predominantly in the medical field, where it could allow in-the-field patient evaluation and thus dramatically decrease both the time of response and the costliness of NMR imaging techniques. Several groups have developed portable or inside-out NMR sensors for a variety of relaxation and imaging studies [1–11]. Roughly concurrently, a series of ex situ methodologies [12,13] and hardware engineering [14,15] has allowed for high resolution spectroscopic information despite the inhomogeneities inherent to such systems. However, volume imaging of large objects with transportable and open instruments has not been pursued.

Numerous important considerations arise during the design of an ex situ volume imaging system. These include the magnet, RF, and gradient coil designs, as well as the pulse sequence optimization for the specific application. Volume imaging requires a magnet with a large, relatively homogeneous sweet spot. Meanwhile, the imaging gradients and RF field must remain homogeneous over a significant portion of the sample.

This differs significantly from the design scheme of traditional portable and/or single-sided NMR and MRI systems. The latter have either flat field profiles that allow the excitation of thin slices parallel to the surface of the magnet or sweet spots for bulk property measurements. Systems with flat static field profiles can obtain high resolution images along the strong natural gradient of the field [5,6,9,16]. Magnets that rely on careful design or additional shims can produce a relatively homogeneous sweet spot on the order of several parts per thousand [8,10,11].

In this communication, we present an open electromagnet system and employ this system to collect preliminary volume images. While, at this point in time, slice imaging is a highly optimized and successful ex situ imaging technique, we present proof of principle results that introduce another class of standard imaging approaches to portable MR setups. The latter methods currently function adequately and also offer several potential improvements for the field of MR imaging. In addition, we present an unconventional hardware setup that may interest researchers in this field.

## 2. Experimental

The magnet (Fig. 1) consists of several solenoidal copper coils centered around a gap of 13.4 cm, which is stepped to give a curvature that allows for the placement of large samples on top of the magnet. The physical dimensions of the magnet are those of a disk 80 cm in diameter and 15 cm high, which weighs 200 kg. The electromagnet is connected to a high stability, customized power supply, based on a FUG, NTN 1400–350 system. The magnetic field strength can be adjusted by changing the current and/or voltage to the two main coils. For the experiments described in this communication, the current was set to approximately

* Corresponding author. Present address: T2 Biosystems, System Development, 286 Cardinal Medeiros Ave., Cambridge, MA 02141, USA. Fax: +1 617 876 1608.
*E-mail address:* vdemas@t2biosystems.com (V. Demas).

0009-2614/$ - see front matter © 2008 Elsevier B.V. All rights reserved.
doi:10.1016/j.cplett.2008.11.069

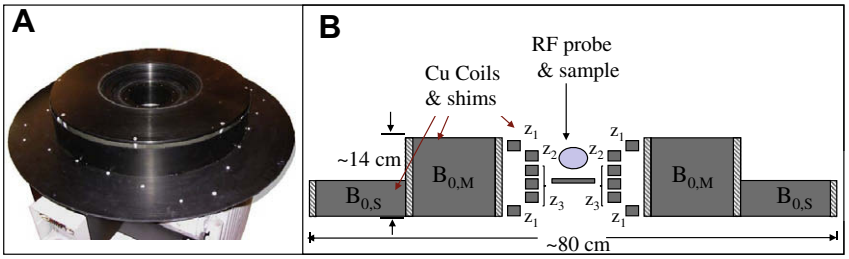


**Fig. 1.** (A) Photograph of the electromagnet. (B) Schematic of a cross section of the magnet. There is cylindrical symmetry. The main and opposing coils are shown, as well as additional solenoid coils used to provide axial shimming fields. The currents through the main coil and the opposing coil ($B_{0,M}$ and $B_{0,S}$) were set to constant values while four additional controls send current through the shim coils. The latter values were optimized for line narrowing.

1.6 Amps, resulting in a voltage of 236 V and a field of approximately 250 G. Adjustments in the power can allow variable field testing of MR parameters. For example, we have used variations of the field to measure fluorine and proton signals with the same RF electronics. The system runs at 45 °C and a combination of conduction and radiation cools the solenoids. Higher fields can be attained with larger amounts of power if the magnet is cooled more effectively, though this would also decrease the transportability of the system. Variable order shims along the $z$ direction can be adjusted by changing the current strength and polarity in the remaining coils. By adjusting a total of four magnet shims (Fig. 1B) we were able to achieve a linewidth of 100 ppm over a cylinder of 1 cm radius and 1 cm height. The magnet design includes space for radial shims; however, radial shim coils were not used at this stage. The magnet was custom-built by MTech Laboratories, and further details on its design and operation can be found in Ref. [17].

The RF probe, built in collaboration with Quantum Magnetics, employs a surface coil that covers the magnet gap and excites volumes of up to several cubic centimeters in size. An RF excitation pulse generated by this probe ($^1$H 90° time is 10 μs) easily excites the resulting spread in resonance frequencies. The coil is a five turn single-sided, double-D design. It provides a field along the $x$-axis along the diameter of the electromagnet, with a sweet spot 1 cm away from the surface of the coils and 1 cm distance along the $z$-axis (away from the surface of the coil). Within an $xy$ slice, the RF field is constant for a small radius (0.5–1 cm), and the main RF gradient points away from the coil along the $z$-direction. A picture of the RF probe and the spatial dependence of the RF field is shown in Fig. 2. An RF excitation pulse generated by this probe ($^1$H 90° time is 10 μs) easily excites the resulting spread in resonance frequencies.

We designed and built two sets of imaging gradients. The first set surrounded the sample and consisted of standard Maxwell and Golay pairs for the $x$- and $y$-gradients. The second set of $x$-, $y$-, and $z$-gradient coils was single sided and placed on top of the RF coil. The $z$-gradient consisted of a multi-turn, compressed solenoid 3 cm in diameter. The $x$ gradient consisted of 4 × 6 cm, 20 step double ladder coils [18]. The field for the latter set of coils only varies linearly over a small region (on the order of 1 cm along the direction of the gradient); there is an inherent $z$ dependence on these lateral gradients, as discussed in Ref. [18], which was not compensated for in these experiments. A schematic depicting both sets is shown in Fig. 3.

The customized spectrometer, built by Quantum Magnetics, operates over a frequency range from 100 kHz to 20 MHz; the current system is tuned to 1 MHz, the proton Larmor frequency at 250 G. The spectrometer box consists of a standard-sized PC running a real time OS. The PC contains an added unit with BNC outputs that control two independent gradient coils, in addition to RF amplitude and phase modulation. Complex, multidimensional experiments, such as those employed here, employ additional software, written by the authors and layered on top of the basic spectrometer software. We developed Python scripts to run multidimensional experiments, Perl scripts for fast data transferral, and Matlab scripts for data processing. The two channel gradient control available in this system forced the use of projection reconstruction for a full volume image. We developed Python scripts to run multidimensional experiments and Matlab scripts for data processing. For a more detailed description of the spectrometer, pulse sequence and processing libraries see Refs. [17,19].

## 3. Results

As described in the previous section, two sets of gradient coils were built. The first set surrounds a sample positioned 1 cm above the RF coil. The second set rests on top of the RF coil; in this instance the sample is placed 2 cm away from the surface of the RF coil. The distances and physical dimensions of the sample are shown in Fig. 4A and Fig. 4B.

We employed a pulse sequence consisting of frequency and phase encoding, augmented by a CPMG train for signal averaging. The 5.5 G/cm frequency encoding gradient was applied along the

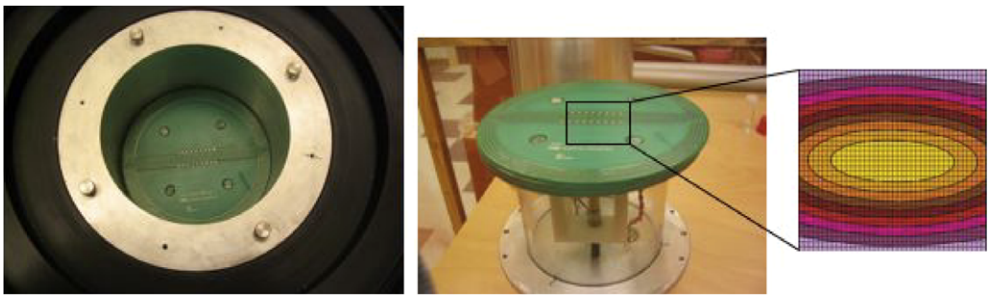

**Fig. 2.** The magnet has a 108 mm gap, where the probe is placed. The RF probe is single sided, and the overall system is open, allowing large sample access. The sweet spot of the probe is in the same spacial location as the sweet spot of the electromagnet, satisfying a 3D 'matching' condition.

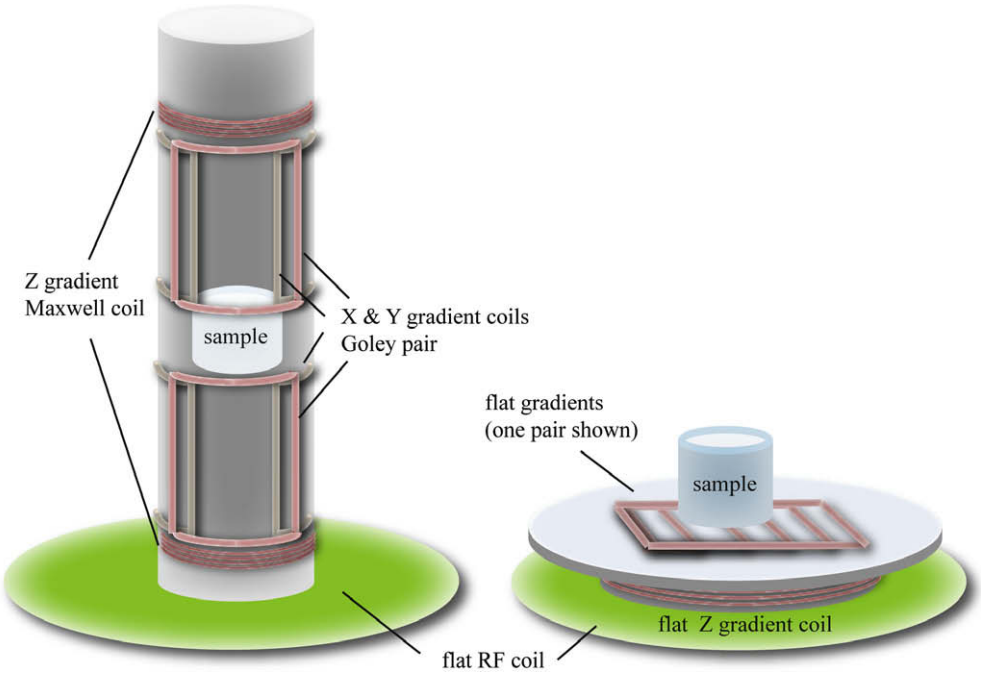


**Fig. 3.** Schematic of the gradient coils. On the left, the first set is shown. The coils are built on a cylinder surrounding the sample and consist of a standard Maxwell pair for the *z* gradient and Golay pair for the *x* and *y* gradients. The second set is single sided and is placed on top of the RF coil. A multiturn loop produces the *z* gradient, and a double ladder coil produces the *x* gradient.

*z*-direction, while the phase encoding gradient was applied along the radial direction up to a maximum strength of 5 G/cm.[1] The phases of the refocusing pulses remain constant, while the phase of the excitation pulse was cycled in 90° steps between scans. As described in Ref. [19], the spectrometer saves signal from all the steps separately to allow access to signal corresponding to different changes in coherence during the excitation pulse, $\Delta c$. For perfect pulses, the spin echo signal occurring in the even and odd echoes would arise from two distinct coherence pathways, corresponding to a $\Delta c$ of $-1$ and +1, respectively, during the excitation pulse. In the event of a single failure to invert, the spins will maintain the given coherence level for two echo periods. In the case where the echo is off-centered, this would also result in the superposition of echoes with two different echo center times for all echo periods after the first echo. However, signal filtered for the proper $\Delta c$ during the excitation pulse suppresses this artifact and exhibits only the echo center time expected for proper inversions. This method demonstrates promise for the filtering of signal under imperfect conditions, as well as detailed processing of 2D spectroscopic J-coupling signal. Note that this method includes use of both the CP and CPMG components of the signal [20].

A volume image of a cylindrical, undoped tap water sample with an oblique separation along the center was obtained with the standard (enclosing) gradient coils. Frequency encoding was applied along the *z*-direction, while phase encoding was applied in a radial direction. The sample was then rotated by 20° and another projection was obtained. For each 2D experiment 600 scans with 0.8 s repetition delay were averaged, while one hundred echoes were saved separately and post processed in MATLAB.[2] We used 43 phase encoding steps and acquired 64 points per echo separated by a 20 μs dwell time. The experimental time for a 2D image was 20 min, corresponding to about 2.5 h for the full 3D image (with

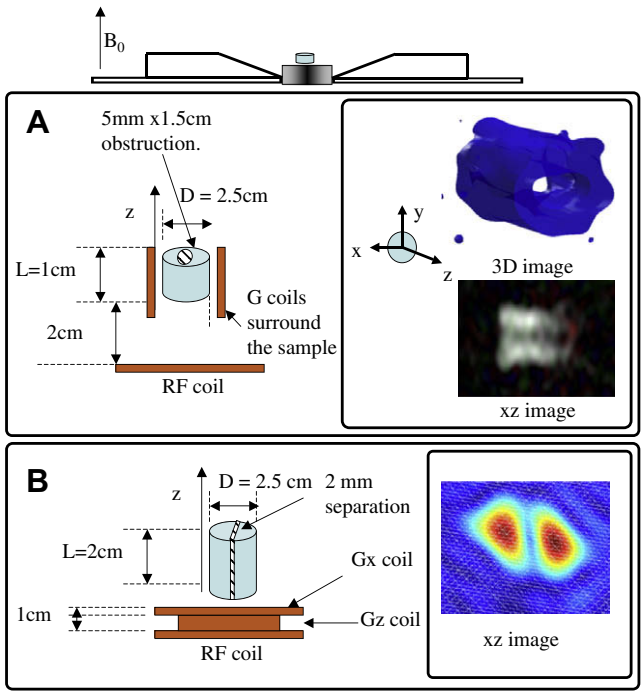


**Fig. 4.** Experimental set-up. (A) First conventional Golay and saddle coils are used to provide gradients along the field and the transverse plane. 3D imaging is accomplished by sample rotation and projection reconstruction. A water sample in a cylinder of 2.5 cm diameter and 1 cm length with an oblique obstruction is imaged. The sample was 2 cm away from the RF coil. (B) Single-sided gradient coils were positioned on top of the RF coil. The *z* coil is a compressed solenoid, while the *x* gradient is a ladder coil, as described in reference [18]. The sample is contained in a cylinder of 2.5 cm diameter and 2 cm length with a 2 mm teflon wall separation in the center.

eight projections) shown in Fig. 4A. The FOV of this image was 4.3 × 4.3 cm and the voxel size was 0.7 × 1 mm and was set to be

[1] Only two gradient control was available in the spectrometer.

[2] The SNR – approximately 7 – can be improved, when a matched filter is used during processing.

larger than the resolution limit as determined by $T_2^*(0.4\ \mathrm{mm}^2)$. In addition to the 3D data, we show an *xz* slice image for reference purposes.

For the open gradient coil configuration, the FOV and resolution were identical to that used with the standard gradient coils. An *xz* image was obtained with the same pulse sequence at 520 points per scan and 2.5 μs dwell time. This experiment imaged a cylindrical sample, 2.5 cm in diameter and 2 cm in height, which contained a teflon wall separation. The sample was placed on top of the gradient coils, and a spacer, 1 cm away from the RF coil surface. Fig. 4B contains the resulting image. One needs to include gradient corrections by hardware additions, as those described in Ref. [18] or via ex situ methodologies as those in Ref. [13].

## 4. Conclusions

Existing single-sided systems, such as the NMR MOUSE and its descendants (e.g. the exo-MRI and the profiler), have been used extensively for imaging experiments [3,8–11]. These systems, however, can only perform slice selective imaging experiments along the extremely high field gradients away from the surface of the magnet; great effort goes towards designing magnets with flat surface profiles for such experiments. The approach demonstrated here differs, aiming to produce full volume images rather than remaining restricted to a series of two dimensional slice images parallel to the surface of the magnet. Such volume imaging presents several advantages over slice imaging.

A feasible implementation of ex situ volume MR imaging will require a decrease in acquisition time. The experiment shown here requires twenty minutes per 2D projection and 2.5 h for a 3D image of a medium sized sample at modest resolution. The need for such a lengthy experiment time arises primarily from a low signal-to-noise ratio (SNR), since the thermal polarization is low at low field strengths. While the demonstrated image resolution is much lower than that of the state of the current art in single-sided units, as described in Refs. [21,22], this should not reflect unfavorably on images acquired without slice selection. The experiments demonstrated here prove the feasibility of a family of alternative imaging methodologies, which offer great promise both for acquiring larger signals from larger volumes of spins and for taking full advantage of the abilities of corrective pulses ([12,13,23,24]) over those volumes. Furthermore, several approaches to increasing the SNR exist, such as hyperpolarization, and could potentially facilitate the acquisition of high SNR images even at the field strengths employed here. The design shown here could be extended/converted to a superconducting magnet, thus indicating that it may be possible to acquire ex situ images and analyze large samples at very high field strengths. For instance, if such a design alteration was implemented on the current system, increasing the static field to a standard clinical instrument field of 1.2 T, the SNR would increase by a factor of approximately 2300.[3] The increased signal to noise in such a setup could not only allow a dramatic speedup of the acquisition time, but would also allow the acquisition of signal in the presence of stronger imaging gradients, thus leading to higher resolution images.

We also anticipate that this experiment will set the stage for further research into the design of corrective pulse sequences. Even thoughtful magnet design can yield single-sided devices with large regions of modest static field gradient. Therefore, even at the rudimentary stages demonstrated here, consideration of the pulse design proves beneficial; namely, when the RF frequency matches the resonance frequency far from the surface of the coil, the frequency offset will be small where the RF field strength is weak, while close to the surface of the coil, where the excitation suffers from a large frequency offset, the strong RF field can compensate for the large offset. While this is the only advantage we used in these experiments, specially designed pulses that operate uniformly over large regions of offsets and RF values, while taking advantage of the existing hardware matching can be designed [19,25].

[3] Based on the $B_0^2$ scaling.

## Acknowledgements

The work described in this Letter was supported by the Director, Office of Science, Office of Basic Sciences, Materials Sciences Division of the US Department of Energy contract No. DE-AC03-76SF0098 and was performed at the University of California, Berkeley and Quantum Magnetics.

## References

[1] W.E. Kenyon, J.J. Howard, A. Sezinger, C. Straley, A. Matteson, K. Horkowitz, R. Ehrlich, Pore size distribution and NMR in microporous cherty sand-stones, in: Transactions of the SPWLA 30th Annual Logging Symposium, Denver, Colorado, USA, 1989.
[2] R. Freedman, C.E. Morriss, Processing data from an NMR logging tool, in: Presented at the 70th SPE Annual Technical Conference and Exhibition, Dallas, Texas, USA, 1995.
[3] G. Eidmann, R. Savelsberg, P. Blümer, B. Blümich, J. Magn. Reson. A 122 (1996) 104.
[4] E. Fukushima, J. Jackson, The NMR News Lett. 490 (1999) 40.
[5] P.J. Prado, J. Magn. Reson. Imaging 21 (2003) 397.
[6] F. Casanova, B. Blümich, J. Magn. Reson. 163 (2003) 38.
[7] H. Raich, P. Blümler, Magn. Reson. Eng. B 23B (1) (2004) 16.
[8] B. Manz, A. Coy, R. Dykstra, C.D. Eccles, M.W. Hunter, B.J. Parkinson, P.T. Callaghan, J. Magn. Reson. 183 (2006) 25.
[9] P.J. McDonald, P.S. Aptaker, J. Mitchell, M. Mulheron, J. Magn. Reson. 185 (2007) 1.
[10] A.E. Marble, I.V. Mastikhin, B.G. Colpitts, B.J. Balcom, J. Magn. Reson. 186 (2007) 100.
[11] J.L. Paulsen, L.S. Bouchard, J. Frank, V. Demas, IEEE Trans. Magnet. 44 (12) (2008).
[12] C.A. Meriles, D. Sakellariou, H. Heise, A.J. Moule, A. Pines, Science 293 (2001) 82.
[13] D. Topgaard, R.W. Martin, D. Sakellariou, C.A. Meriles, A. Pines, Proc. Natl. Acad. Sci. USA 101 (2004) 17576.
[14] J. Perlo, V. Demas, F. Casanova, C. Meriles, J. Reimer, A. Pines, B. Bluemich, Science 308 (2005) 1279.
[15] J. Perlo, F. Casanova, B. Bluemich, Science 315 (2007) 5815.
[16] P.J. Prado, B. Blümich, U. Schmitz, J. Magn. Reson. 144 (2000) 200.
[17] V. Demas, Ex situ NMR: Single Sided and Portable Magnetic Resonance Sensors, Ph.D. Thesis, UC Berkeley, 2006.
[18] V. Demas, C. Meriles, D. Sakellariou, S. Han, J. Reimer, A. Pines, Concept. Magnetic. Res. B 29B (2006) 137.
[19] J. Franck, The Design and Testing of RF Pulses to Encode Compensations and Perform Excitations in Inhomogeneous Fields Ph.D. Thesis, UC Berkeley, 2008.
[20] J. Perlo, F. Casanova, B. Blümich, J. Magn. Reson. 173 (2005) 254.
[21] J. Perlo, F. Casanova, B. Blümich, J. Magn. Reson. 166 (2004) 228.
[22] F. Casanova, J. Perlo, B. Blümich, J. Magn. Reson. 166 (2004) 76.
[23] C.A. Meriles, D. Sakellariou, A. Pines, J. Magn. Reson. 164 (2003) 177.
[24] V. Demas, D. Sakellariou, C. Meriles, S. Han, J. Reimer, A. Pines, Proc. Natl. Acad. Sci. USA 101 (24) (2004) 8845.
[25] K. Kobzar, B. Luy, N. Khaneja, S.J. Glaser, J. Magn. Reson. 173 (2005) 229.